SUPPLEMENTAL MATERIAL

Drumm et al., https://doi.org/10.1085/jgp.201711771

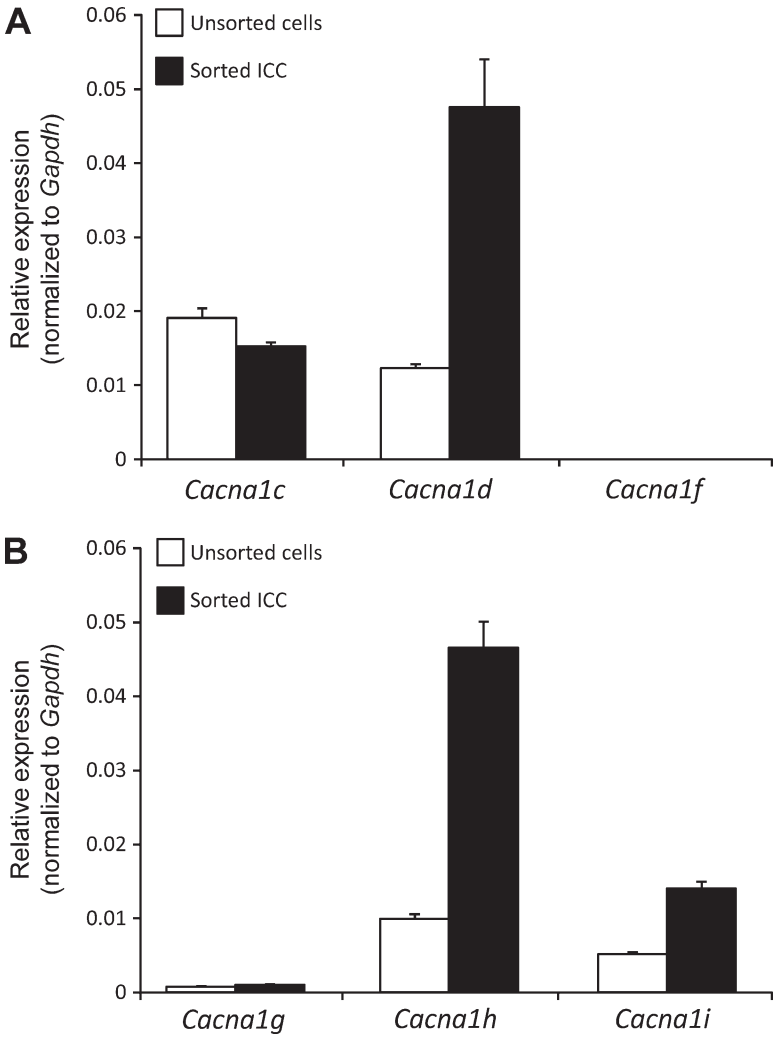

Figure S1. **Molecular expression of voltage-dependent Ca^{2+} channels (L- and T-type) transcripts in ICC.** (A) Relative expression of L-type Ca^{2+} channel isoforms (*Cacna1c*, *Cacna1d*, and *Cacna1f*) in sorted ICC and in unsorted cells (i.e., mixed cell population after enzymatic dispersions of jejunal muscles) as determined by qPCR. Transcripts of L-type Ca^{2+} channel isoforms *Cacna1c* and *Cacna1d* were resolved in sorted ICC; however, the highest isoform expressed in ICC was *Cacna1d*. *Cacna1f* expression was not resolved in ICC. (B) Relative expression levels of T-type Ca^{2+} channel isoforms (*Cacna1g*, *Cacna1h*, and *Cacna1i*) in sorted ICC in comparison with unsorted cells. The relative expression of each gene was normalized to the house-keeping gene, *Gapdh*. The data are plotted with as mean ± SEM and derived from experiments on four tissues of four animals that were dispersed and sorted separately, and then qPCR was performed on each individual sample.

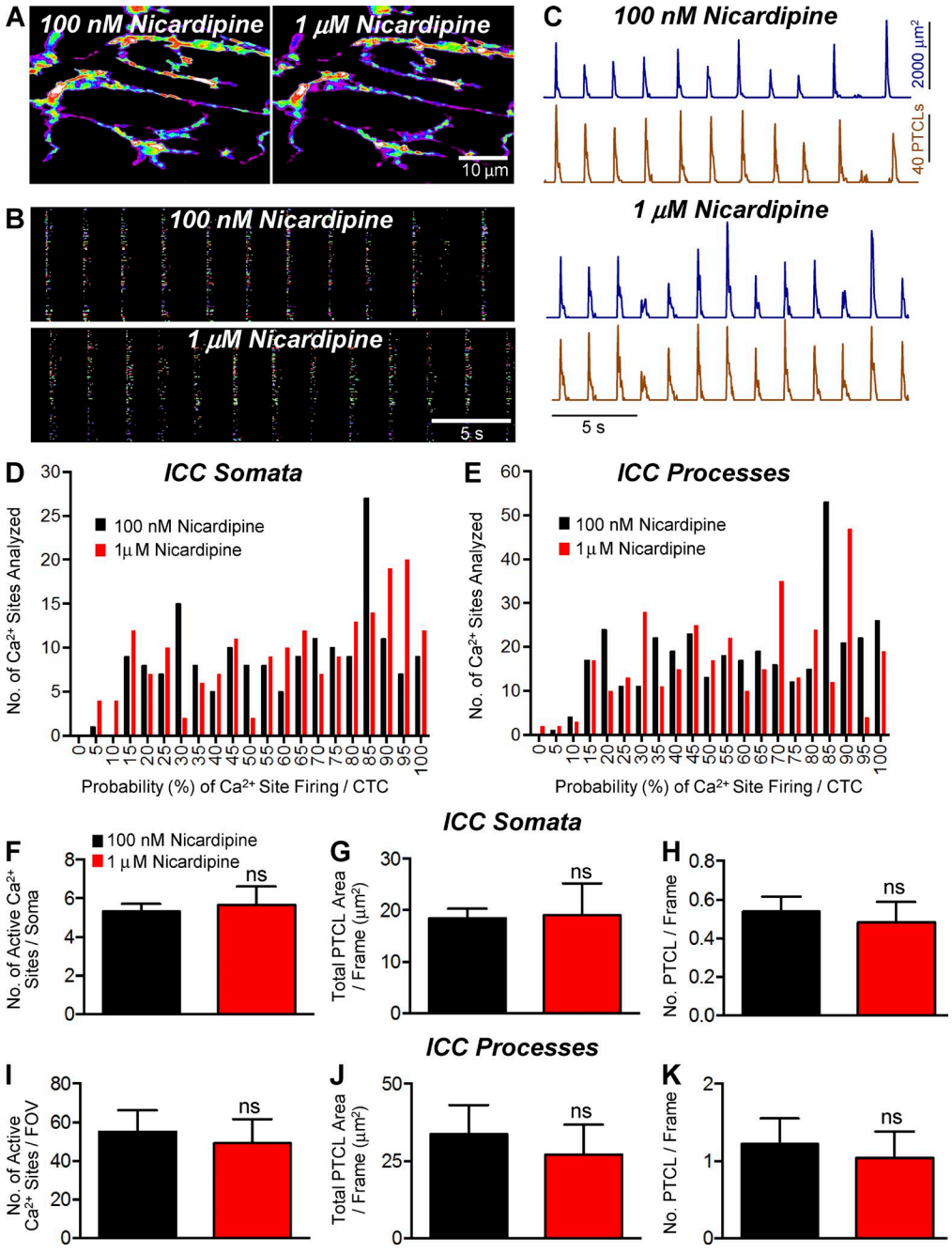

Figure S2. **The effect of nicardipine on Ca^{2+} transients in ICC-MY.** (A) Representative heat map showing the summated PTCLs of ICC-MY in control (100 nM nicardipine) and 1 μM nicardipine. (B) Occurrence map of individually color coded Ca^{2+} firing sites in the ICC-MY network in control and 1 μM nicardipine conditions. (C) Traces of PTCL activity over an entire recording of the ICC-MY network in control conditions and in the presence of nicardipine (1 μM) showing PTCL area (dark blue) and PTCL count (brown). (D and E) Histogram showing the probability (%) that an individual Ca^{2+} firing site in the ICC-MY cell soma and cell processes in E will fire during a CTC cycle in the presence of nicardipine (1 μM; red bars) compared with control conditions (black bars; n = 5, FOV = 7). (F) Summary showing that the number of Ca^{2+} firing sites in cell soma was not significantly affected by nicardipine (1 μM; P = 0.59). (G) PTCL area/frame in the cell soma was 18.4 ± 1.8 μm² in control and 19 ± 6.2 μm² in nicardipine (1 μM; P = 0.92, n = 5, FOV = 7). (H) The PTCL count/frame in the cell soma was 0.5 ± 0.08 in control and 0.5 ± 0.1 in nicardipine (1 μM; P = 0.57, n = 5, FOV = 7). (I) The number of Ca^{2+} firing sites in the cell processes per FOV changed from 55 ± 11.1 in control to 49.4 ± 12.5 in nicardipine (1 μM; P = 0.29, n = 5, FOV = 7). (J) PTCL area/frame in the cell processes was 33.6 ± 9.5 μm² in control and 27.1 ± 9.7 μm² in nicardipine (1 μM; P = 0.19, n = 5, FOV = 7). (K) The PTCL count/frame in the cell processes was 1.2 ± 0.3 in control and 1 ± 0.3 in nicardipine (1 μM; P = 0.12, n = 5, FOV = 7). ns, P > 0.05. Mean ± SE is shown.

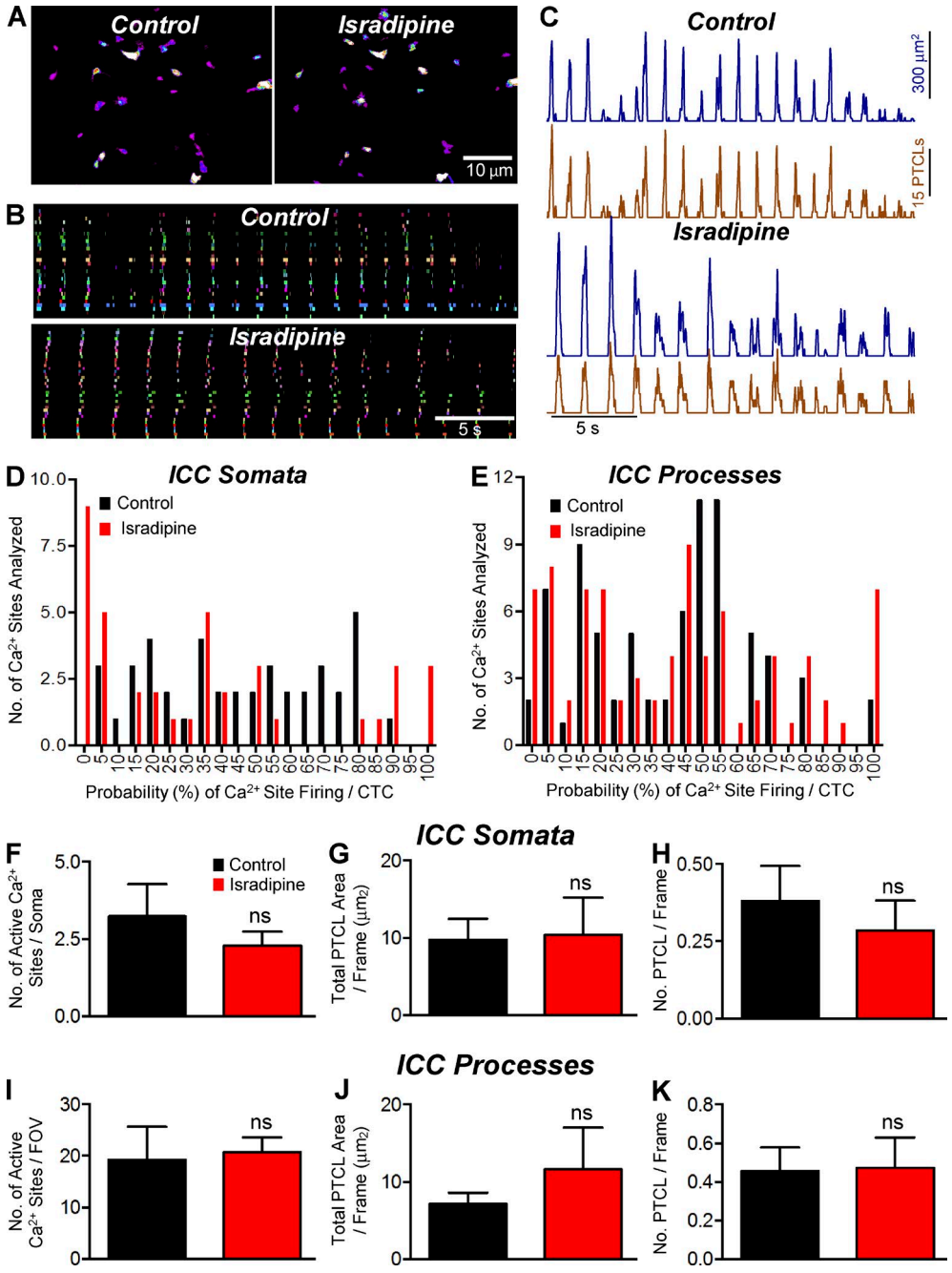

Figure S3. **The effect of isradipine on Ca^{2+} transients in ICC-MY.** (A) Representative heat map showing the summated PTCLs of ICC-MY in control and 1 µM isradipine. (B) Occurrence map of individually color-coded Ca^{2+} firing sites in the ICC-MY network in control and isradipine conditions. (C) Traces of PTCL activity over an entire recording of the ICC-MY network in control conditions and in the presence of isradipine (1 µM) showing PTCL area (dark blue) and PTCL count (brown). (D and E) Histogram showing the probability (%) that an individual Ca^{2+} firing site in the ICC-MY cell soma and cell processes in E will fire during a CTC cycle in the presence of isradipine (1 µM; red bars) compared with control conditions (black bars; n = 4, FOV = 4). (F) Summary showing that the number of Ca^{2+} firing sites in cell soma was not significantly affected by isradipine (1 µM; P = 0.43). (G) PTCL area/frame in the cell soma was 9.8 ± 2.7 µm^2 in control and 10.4 ± 4.9 µm^2 in isradipine (1 µM; P = 0.91, n = 4, FOV = 4). (H) The PTCL count/frame in the cell soma was 0.4 ± 0.1 in control and 0.3 ± 0.09 in isradipine (1 µM; P = 0.57, n = 4, FOV = 4). (I) The number of Ca^{2+} firing sites in the cell processes per FOV changed from 19.3 ± 6.4 in control to 20.75 ± 2.8 in isradipine (1 µM; P = 0.83, n = 4, FOV = 4). (J) PTCL area/frame in the cell processes was 7.1 ± 1.4 µm^2 in control and 11.6 ± 5.4 µm^2 in isradipine (1 µM; P = 0.45, n = 4, FOV = 4). (K) The PTCL count/frame in the cell processes was 0.46 ± 0.1 in control and 0.5 ± 0.16 in isradipine (1 µM; P = 0.93, n = 4, FOV = 4). ns, P > 0.05. Mean ± SE is shown.

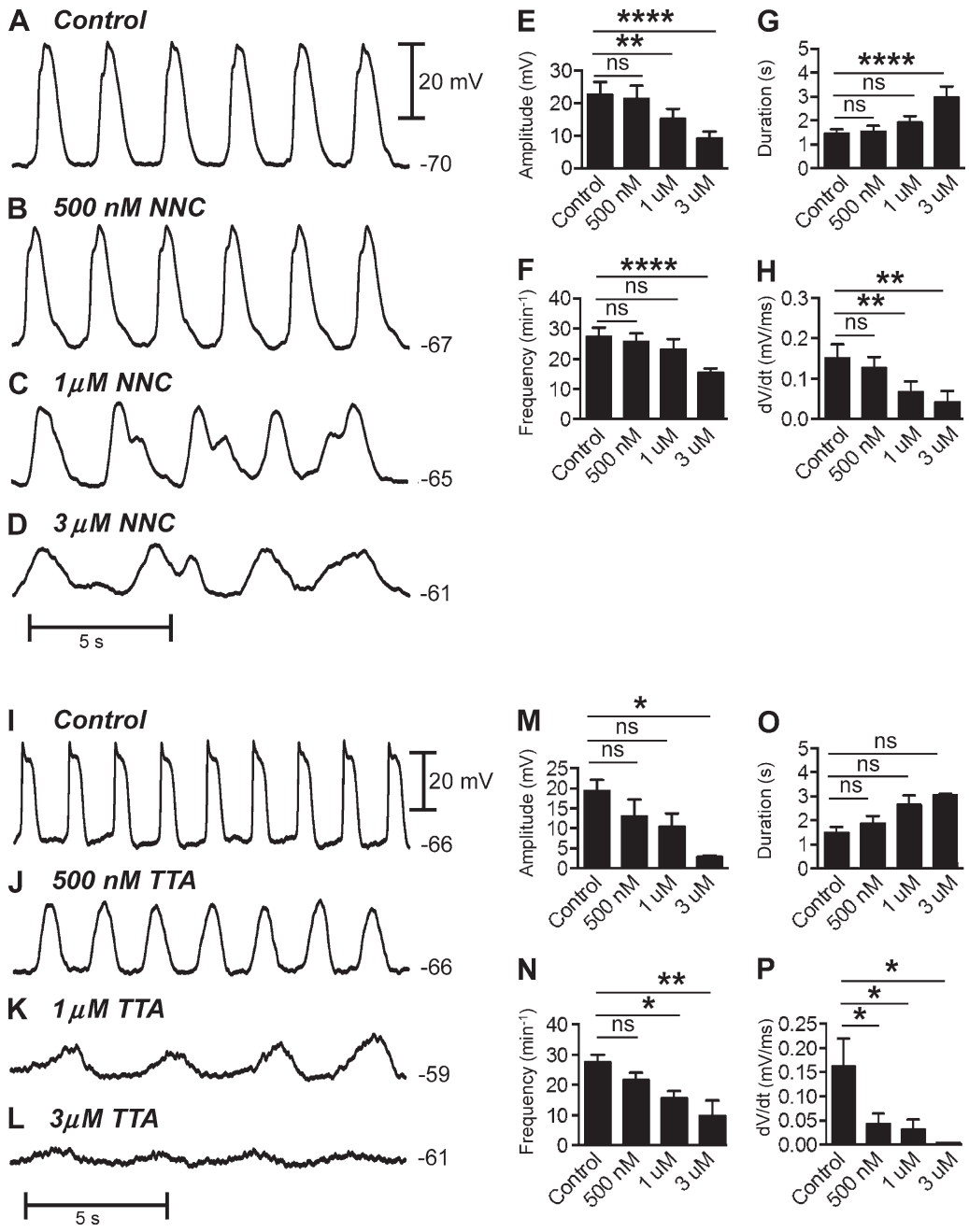

Figure S4. **The effect of the T-type Ca^{2+} channel blockers on electrical slow wave activity.** (A) Representative recording from small intestine muscles displaying spontaneous electrical slow waves. (B–D) Representative traces showing the effect of 500 nM NNC 55-0396 (B), 1 μM NNC 55-0396 (C), and 3 μM NNC 55-0396 (D) on slow waves. Note that the time scale in D and the amplitude scale in A pertain to A–D. (E–H) Summary data showing the effect of increasing concentrations of NNC 55-0396 on slow wave amplitude (mV), frequency (min^{-1}), duration (s), and dV/dt (mV/ms), respectively (n = 5). (I) Representative electrical recording of jejunal slow waves. (J–L) Representative traces showing the effect of TTA-A2 on slow waves at 500 nM (J), 1 μM (K), and 3 μM (L). The time scale in L and the amplitude scale in J pertain to L–J. (M–P) Summary data showing dose response relationships of the effect of increasing concentrations of TTA-A2 on slow wave amplitude (mV), frequency (min^{-1}), duration (s), and dV/dt (mV/ms; n = 6). ns, P > 0.05; *, P < 0.05; **, P < 0.01; ****, P < 0.0001. Mean ± SE is shown.

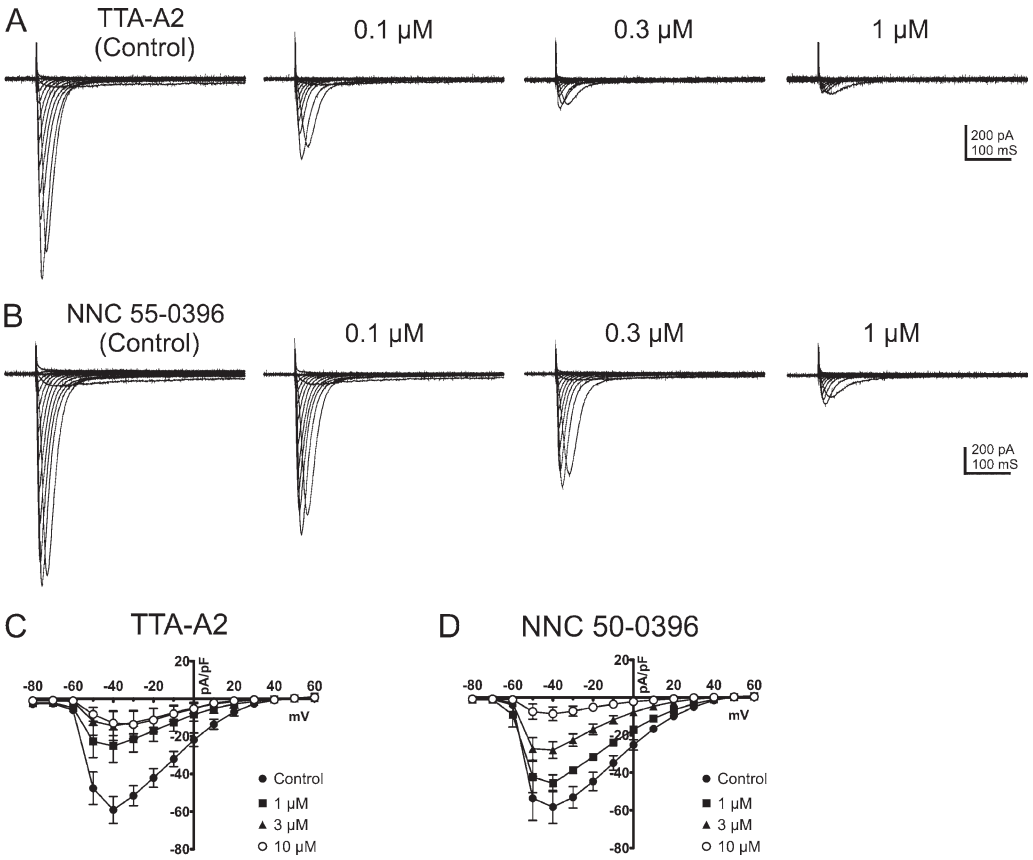

Figure S5. **Effects of T-type Ca^{2+} channel blockers on $Ca_V3.2$ currents.** (A) Representative traces showing TTA-A2 effects on $Ca_V3.2$ currents in HEK293 cells. Currents were evoked by step protocol from −80 to 60 mV in 10-mV increments from a holding potential of −80 mV. (B) Representative traces showing NNC 55–0396 effects on $Ca_V3.2$ currents in HEK293 cells. Currents were evoked by step protocol from −80 to 60 mV in 10-mV increments from a holding potential of −80 mV. (C and D) Current-voltage (I-V) relationships for $Ca_V3.2$ currents was normalized to cell size (pF) in the presence of TTA-A2 (C) and NNC 55-0396 (D). Results from five cells are displayed as means ± SEM.

Table S1. **Quantifying the effects of nicardipine on CTCs in ICC-MY**

CTC parameters	100 nM NICRD	1 μM NICRD	3 μM NICRD
Probability (%) of Ca^{2+} site firing/CTC cycle (soma)	60.4 ± 2	62.4 ± 2.1	40.7 ± 2.6
Probability (%) of Ca^{2+} site firing/CTC cycle (processes)	61 ± 1.4	55.5 ± 1.5	32.9 ± 1.7
No. of Ca^{2+} sites/soma	5.3 ± 0.4	5.7 ± 0.9	4.3 ± 1.2
No. of Ca^{2+} sites/process FOV	55 ± 11.1	49.4 ± 12.5	39.1 ± 11.3
PTCL area/frame (μm^2) soma	18.4 ± 1.8	19 ± 6.2	10.2 ± 4.7
PTCL area/frame (μm^2) processes	33.6 ± 9.5	27.1 ± 9.7	14.2 ± 5.4
PTCL count/frame soma	0.5 ± 0.08	0.5 ± 0.1	0.3 ± 0.1
PTCL count/frame processes	1.2 ± 0.3	1 ± 0.3	0.6 ± 0.2

Table S2. **Summary of gene primers for L- and T-type voltage gated Ca^{2+} channels**

Gene	Primer sequence (5′-3′)	GenBank accession number
Cacna1a-F	CCTCATCATCATCGGCTCCT	NM_007578
Cacna1a-R	CGCAAGAATCACCTCTTCTGC	NM_007578
Cacna1c-F	GTAAGGATGAGTGAAGAAGCCGAGTAC	NM_009781
Cacna1c-R	CAGAGCGAAGGAAACTCCTCTTTGG	NM_009781
Cacna1d-F	ACCAAAGAAACAGAAGGCGG	NM_028981
Cacna1d-R	TGTAAACTGGGCACTCCTGA	NM_028981
Cacna1f-F	AGCCCTCCTCACTGTCTTTC	NM_019582
Cacna1f-R	TCAGCAGGATGTAGTTGCCA	NM_019582
Cacna1g-F	ACAACGGCATGGCCTCCACGT	NM_009783
Cacna1g-R	CCGTTTGCCGATTTCCTCTGCCTG	NM_009783
Cacna1h-F	TGGAGACCTACACAGGCCCGGT	NM_021415
Cacna1h-R	CAGAGAGCGGGGCGTATCC	NM_021415
Cacna1i-F	CTGTGCCTCGTTGTCATAGC	NM_001044308
Cacna1i-R	ATCTCCTCATAGCAGTCGCC	NM_001044308

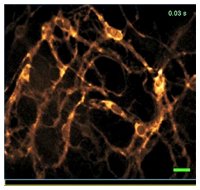

Video 1. **Ca^{2+} waves propagating through an ICC-MY network in murine small intestine.** The video shows Ca^{2+} waves propagating through an ICC-MY network in murine jejunum expressing the genetically encoded Ca^{2+} indicator GCaMP3. The FOV shows a network of stellate-shaped ICC-MY imaged with a 20× objective. A brown hue was added as an overlay to enhance visualization; color scale indicates intensity of Ca^{2+} transients (i.e., dark brown is low florescence; light yellow to white indicate high florescence levels). Video playback is set at 15 fps (approximately half the acquisition rate) to allow better visualization of Ca^{2+} wave propagation. The green scale bar is 25 µm.

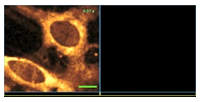

Video 2. **Spontaneous Ca^{2+} transients in ICC-MY.** This video shows enhanced resolution of Ca^{2+} transients in ICC-MY expressing the genetically encoded Ca^{2+} indicator GCaMP3. The left FOV shows stellate-shaped ICC-MY imaged with a 60× objective. A brown hue was added as an overlay to enhance visualization; color scale indicates intensity of Ca^{2+} transients (i.e., dark brown is low florescence; light yellow to white indicates high florescence levels). The green scale bar is 5 µm. The right FOV shows the Ca^{2+} particle (PTCL) file, color coded in blue for raw PTCLs, and the centroids of particles are indicated in purple. Note the asynchronous, multiple-site firing of Ca^{2+} transients in ICC-MY. The Ca^{2+} transients were organized into CTCs, as explained in the Materials and methods and Results. CTCs originated after a short delay after the upstroke depolarization of slow waves, suggesting that Ca^{2+} transients at multiple sites were entrained into CTCs by a voltage-dependent mechanism. The video shows several successive CTCs traversing the FOV. Asynchronous firing of Ca^{2+} transients during CTCs results in sustained elevation of $[Ca^{2+}]_i$ creating the plateau phase of slow waves. Video playback is set at 50 fps (approximately half the acquisition rate) to allow better visualization of CTCs.